Effect of Polymer Architecture of Amphiphilic Poly(2-oxazoline) Copolymers on the Aggregation and Aggregate Structure

Tune B. Bonné, Karin Lüdtke, Rainer Jordan,* Christine M. Papadakis*

The micelle formation of five poly(2-oxazoline) diblock, triblock and gradient copolymers in water was investigated using fluorescence correlation spectroscopy. The polymers were synthesized by consecutive or simultaneous living cationic polymerization of 2-methyl-2-oxazoline for the hydrophilic and 2-nonyl-2-oxazoline for the hydrophobic polymer segments. Fractions of the polymers were fluorescence-labeled at the polymer termini with TRITC for the FCS measurements. The hydrodynamic radii of solubilized polymer unimers and of the aggregates (micelles) were determined in a concentration range of 10^{-8}–10^{-3} M and were found to depend in a characteristic way on the polymer architecture.

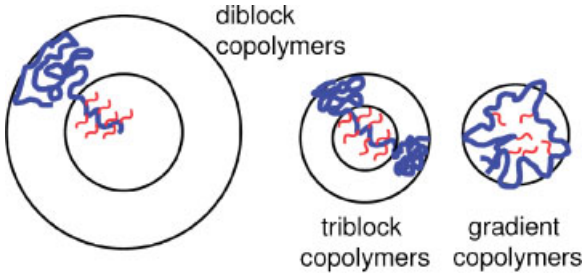

Introduction

Micelle formation is frequently encountered in amphiphilic block copolymers in aqueous solution.[1–3] The critical micelle concentrations (CMC's) are typically low (10^{-8}–10^{-2} M),[4–7] and above this concentration, micelles of core-shell type are formed. The architecture of the block copolymers (e.g. diblock, triblock or random copolymers) has a strong influence on the micelle formation and on the size of the micelles, because of the steric situation the polymer may encounter to optimize the hydrophobic interaction and entropic contributions due to block or segment stretching/coiling. However, in many investigations, only single samples were studied, and a systematic investigation of the aggregation behavior as a function of the polymer architecture is rare. We present here results from a study of poly(2-oxazoline) copolymers, which offer the possibility to tailor amphiphilic polymers of comparable composition but different polymer architectures. For poly(2-alkyl-2-oxazoline)s, the water-solubility of the monomer units can be controlled by altering the nature of the substitution in the 2-position. In case of *n*-alkyl chains longer than ethyl, the monomer unit is of amphiphilic nature with the structure of a non-ionic polysoap with a polar backbone and a water-insoluble side group. However, long alkyl side-chains also impose steric hindrance to the polymer backbone and force the polymer to stretch as known from 'bottle-brush' type polymers.[8] The aggregation behavior of copolymers containing both, water-soluble and soap-like monomers is thus expected to

T. B. Bonné, C. M. Papadakis
Physik Department E13, Technische Universität München, James-Franck-Str. 1, 85747 Garching, Germany
E-mail: Christine.Papadakis@ph.tum.de
K. Lüdtke, R. Jordan
Wacker-Lehrstuhl für Makromolekulare Chemie, Department Chemie, Technische Universität München, Lichtenbergstr. 4, 85747 Garching, Germany
E-mail: Rainer. Jordan@tum.de

Macromol. Chem. Phys. **2007**, *208*, 1402–1408

DOI: 10.1002/macp.200700140

be more complex than the one of the usual copolymers with water-soluble and water-insoluble monomers.

We have previously found that poly(2-oxazoline) diblock copolymers from methyl-2-oxazoline (MOx) and nonyl-2-oxazoline (NOx) monomers in aqueous solution form micelles, and the critical micelle concentrations (CMC) and the unimer and micellar hydrodynamic radii could be determined using fluorescence correlation spectroscopy (FCS).[9,10] Moreover, using small-angle neutron scattering, we have shown that the micelles are of core-shell type.[11–13] Recently, Weberskirch et al.[14] used triphenylphosphane-functionalized block as well as 'random' copolymers of MOx and NOx as polymer supports in an aqueous two-phase hydroformulation reaction of 1-octene. They reported of a significant difference in the catalytic performance of the functionalized polymer aggregates formed by the amphiphilic random vs. the defined block copolymers, i.e. the random copolymers showed much higher catalytic activities and different *n/iso* selectivities. They attributed this behavior to differences of the aggregation behavior and morphology of the aggregates as well as to a different surface activity of the random block copolymers. Following the early work of Schulz,[15] they performed surface tension measurements with both copolymer types and concluded that, in contrast to block copolymer amphiphiles, the random copolymers are more efficient in the reduction of the surface tension. Here, it is noteworthy that the copolymers investigated by Schulz were derived by true random copolymerization of 2-ethyl-2-oxazoline with 2-heptyl-2-oxazoline, whereas Weberskirch copolymerized 2-methyl-2-oxazoline (MOx) with 2-nonyl-2-oxazoline (NOx). The studies by Schubert et al.[16] on the random copolymerization kinetics of the MOx and NOx monomers and recent own recent kinetic studies on related systems revealed that copolymerizations of MOx with 2-oxazolines having longer side chains do not result in strictly random copolymers with MOx but into copolymers with a *gradient* composition with increased frequency of the 2-oxazoline monomer unit with the longer (more hydrophobic) side chain towards the polymer chain end.[17,18] The more interesting become the findings of Weberskirch et al. on the MOx/NOx copolymer systems in micellar catalysis, since even a gradient system displays enhanced catalytic and surface activity.

In the present publication, we investigate the influence of the copolymer architecture of amphiphilic copolymers of NOx and MOx on the aggregation behavior (CMC) and the micellar hydrodynamic radius of the solubilized unimers and formed aggregates. Both ABA triblock copolymers, polyMOx-*block*-polyNOx-*block*-polyMOx ($PMOx_l$-*b*-$PNOx_m$-*b*-$PMOx_n$), and gradient copolymers polyNOx-*gradient*-polyMOx ($PNOx_m$-*g*-$PMOx_n$) have been investigated using FCS and have been compared to the previously studied AB diblock copolymers, polyNOx-*block*-polyMOx ($PNOx_m$-*b*-$PMOx_n$). In this way, the influence of the position and distribution of the hydrophobic monomer upon the aggregation behavior and structure of the aggregates are explored.

Experimental Part

Synthesis

The synthesis, characterization and fluorescence-labeling of the diblock copolymers have been described in detail in ref.[9]. The characteristics of the diblock copolymers and the tracers are compiled in Table 1. Triblock copolymer synthesis was performed in an analog three-step-one-pot synthesis adding the additional hydrophobic NOx segment. As with the diblocks, the targeted and obtained polymer compositions were in good agreement. The gradient copolymers were synthesized by adding MOx and NOx monomers in one initial monomer feed. All polymerizations were terminated by adding an excess of dry piperazine as described before. Fluorescence labeling with tetramethylrhodamine isothiocyanate (TRITC) of a fraction of the respective polymers were performed accordingly.[9,10]

Table 1. Analytical values of the polymer amphiphiles and results from FCS. The subscripts denote the average degrees of polymerization.

Polymer	$\overline{M}_n$ [a]	PDI[b]	f_{NOx}[c]	r_H^{uni}	r_H^{mic}	CMC
	$g \cdot mol^{-1}$			nm	nm	$10^{-6}\ mol \cdot L^{-1}$
$PMOx_{40}$-*b*-$PNOx_7$[d]	4 034	1.20	0.30	1.4 ± 0.4	13 ± 2	8 ± 2
$PNOx_{10}$-*b*-$PMOx_{32}$[d]	4 796	1.07	0.43	1.3 ± 0.2	11.3 ± 0.9	20 ± 10
$PMOx_{20}$-*b*-$PNOx_7$-*b*-$PMOx_{14}$	4 380	1.40	0.33	1.3 ± 0.3	5.7 ± 0.7	3 ± 2
$PMOx_{30}$-*b*-$PNOx_7$-*b*-$PMOx_{26}$	6 250	1.35	0.23	1.4 ± 0.2	5.6 ± 0.9	2 ± 1
P(MOx_{40}-*g*-NOx_6)	4 690	1.38	0.27	1.2 ± 0.1	4.7 ± 0.3	8 ± 3

[a] From end group analysis of ^1H NMR spectra; [b] Polydispersity index from GPC; [c] Volume fraction of NOx based on the densities 1.06 $g \cdot cm^{-3}$ for pMOx (calculated based on the group contributions[28]) and 0.93 $g \cdot cm^{-3}$ for pNOx.[29]; [d] Results from ref.[9].

Fluorescence Correlation Spectroscopy

A ConfoCor 2 from Carl Zeiss Jena GmbH was used together with a He-Ne laser ($\lambda = 543$ nm), a pinhole with a diameter of 80 μm, a BP 560–615 emission filter and an HFT 543 plate beam splitter. Measurements were conducted at room temperature. The autocorrelation functions of the fluctuations of the fluorescence intensity, $G(\tau)$, were analyzed by fitting the following expression:[19]

$$G(\tau) = 1 + \frac{1}{N}\left(\frac{T_T}{1-T_T}\exp\left(-\frac{\tau}{\tau_T}\right)\right)\sum_{i=1}^{n}\frac{\rho_i}{\left(1+\frac{\tau}{\tau_{D,i}}\right)\sqrt{1+\frac{\tau}{\tau_{D,i}S^2}}} \quad (1)$$

where N is the total number of fluorescent particles in the observation volume, n the number of different fluorescent species, $\tau_{D,i}$ the diffusion time of the i-th species, ρ_i the amplitude of the i-th species, and S the axial ratio of the observation volume given by $S = z_0/w_0$ with z_0 and w_0 the half-height and half-width of the observation volume, respectively. T_T and τ_T are the triplet fraction and time, respectively. From the fit, the values were found to be in the range $T_T = 0.05$–0.15 and $\tau_T = 0.005$–0.01 ms. w_0 was determined before each session by measuring the diffusion time of Rhodamine 6G (Sigma-Aldrich, $D_{Rh6G} = 2.8 \times 10^{-10}\,\mathrm{m^2 \cdot s^{-1}}$, ref.[20]), $\tau_{D,Rh6G}$, and by using $w_0 = (4D_{Rh6G} \times \tau_{D,Rh6G})^{1/2}$. Values $w_0 \approx 0.2$–0.3 μm have typically been obtained. The ratio z_0/w_0 determined from the fit to the Rhodamine 6G correlation functions was typically 5–6. Using the Stokes-Einstein relation together with the viscosity of water at room temperature, 10^{-3} Pa·s, the hydrodynamic radii $r_{H,i}$ corresponding to $\tau_{D,i}$ were calculated.

Stock solutions of fluorescence-labeled and non-labeled polymers were prepared by dissolving the polymers in deionized and filtered water. Prior to mixing solutions from labeled and non-labeled polymers, the solutions of non-labeled polymers were heated to 80 °C for 12 h in order to avoid non-equilibrium aggregates.[9] The FCS measurements were performed at room temperature as previously described.[9]

Results

We have previously reported on FCS measurements on aqueous solutions of labeled and non-labeled diblock copolymers with the compositions $PNOx_{10}$-*b*-$PMOx_{32}$ and $PMOx_{40}$-*b*-$PNOx_7$,[9,10] where the subscripts denote the degree of polymerization. In all measurements, the identical copolymers labeled with TRITC were used as tracers. Here, we present results of the aggregation behavior of two triblock copolymers, $PMOx_{20}$-*b*-$PNOx_7$-*b*-$PMOx_{14}$ and $PMOx_{30}$-*b*-$PNOx_7$-*b*-$PMOx_{26}$, and a gradient copolymer, P(MOx_{40}-*g*-NOx_6).

Triblock Copolymers

Both triblock copolymers under study, $PMOx_{20}$-*b*-$PNOx_7$-*b*-$PMOx_{14}$ and $PMOx_{30}$-*b*-$PNOx_7$-*b*-$PMOx_{26}$, are of ABA type, i.e. they consist of a water-insoluble PNOx middle block and water-soluble PMOx end blocks of approximately equal degree of polymerization (Table 1). In order to investigate the influence of the degree of polymerization of the water-soluble PMOx block on the hydrodynamic radius of the micelles, the length of the PNOx middle block was chosen to be the same in both copolymers (degree of polymerization of seven), and only the length of the PMOx blocks was varied. FCS allowed us to determine the diffusion coefficients of labeled unimers and micelles in aqueous solution covering a wide concentration range (10^{-8}–10^{-3} M).[9] For this purpose, we have used copolymers that were fluorescence-labeled at the terminus with TRITC. Solutions of labeled copolymers having low concentrations (below 10^{-8} M) were mixed with solutions of the non-labeled, identical copolymers. In this

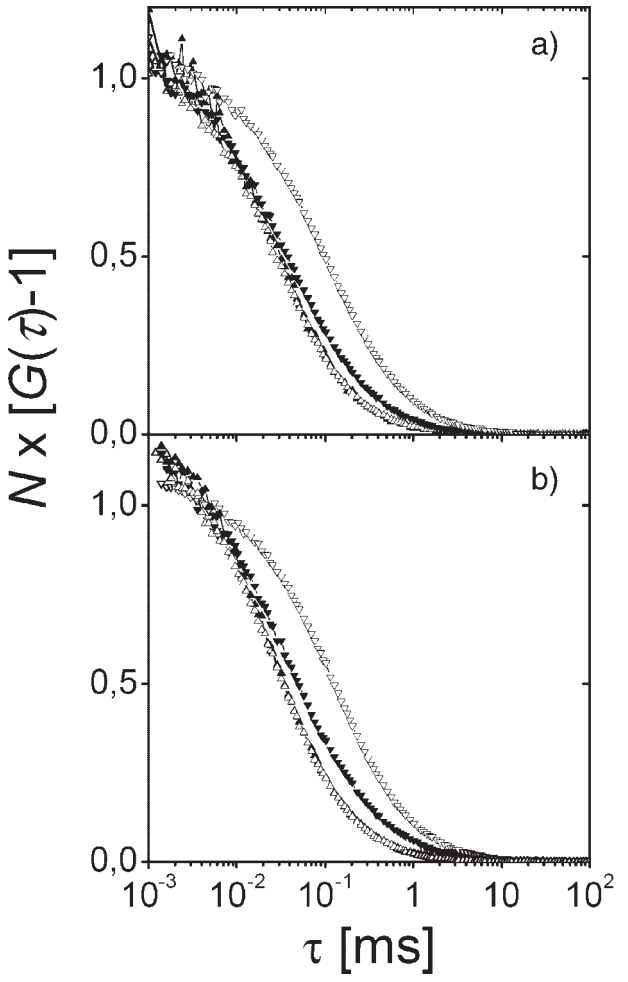

Figure 1. FCS correlation functions of aqueous solutions of the triblock copolymers. (a) $PMOx_{20}$-*b*-$PNOx_7$-*b*-$PMOx_{14}$ at the overall polymer concentrations 1×10^{-8} M (▲), 1×10^{-6} M (△), 1×10^{-5} M (▼) and 6×10^{-4} M (▽). (b) $PMOx_{30}$-*b*-$PNOx_7$-*b*-$PMOx_{26}$ at the overall concentrations 7×10^{-9} (▲), 8×10^{-7} (△), 8×10^{-6} (▼) and 4×10^{-4} (▽). The curves were normalized by the inverse average number of fluorescent molecules in the detection volume, $1/N$, as determined from the fit of Equation (1) to the experimental curves.

Macromol. Chem. Phys. **2007**, *208*, 1402–1408

Macromolecular Journals

DOI: 10.1002/macp.200700140

way, the fluorescence-labeled copolymers served as tracers in the FCS experiment, and we could determine the CMC's as well as the hydrodynamic radii of the unimers and the micelles, r_H^{uni} and r_H^{mic}.

The autocorrelation functions of the shorter triblock copolymer, $PMOx_{20}$-*b*-$PNOx_7$-*b*-$PMOx_{14}$, at concentrations below 3×10^{-6} M show a single diffusional process with a diffusion coefficient of $(1.9 \pm 0.2) \times 10^{-10}$ $m^2 \cdot s^{-1}$ (Figure 1a, 2a). This value is of the same order of magnitude as the one of the diblock copolymers $PMOx_{40}$-*b*-$PNOx_7$ and $PNOx_{10}$-*b*-$PMOx_{32}$[9,10] which have similar degrees of polymerization as the triblock copolymer. We conclude that the diffusional process observed is due to the diffusion of labeled unimers having a hydrodynamic radius of $r_H^{uni} = 1.3 \pm 0.3$ nm (Table 1).

Above a concentration of 3×10^{-6} M, an additional slower diffusional process is present in the autocorrelation functions (Figure 1a, 2a, 2c), in analogy with the behavior of the diblock copolymers.[9,10] We attribute this process to the diffusion of micelles containing fluorescence-labeled unimers. The average diffusion coefficient of the micelles of $(4.3 \pm 0.5) \times 10^{-11}$ $m^2 \cdot s^{-1}$ corresponds to a hydrodynamic radius of $r_H^{mic} = 5.7 \pm 0.7$ nm. The concentration of 3×10^{-6} M is attributed to the CMC. It is of the same order as the one of the diblock copolymers studied previously.

Very similar behavior is observed for the other triblock copolymer, $PMOx_{30}$-*b*-$PNOx_7$-*b*-$PMOx_{26}$, having longer hydrophilic blocks (Figure 1b, 2b, 2d). The average diffusion coefficients of the labeled unimers and micelles are $(1.8 \pm 0.4) \times 10^{-10}$ $m^2 \cdot s^{-1}$ and $(4.4 \pm 0.7) \times 10^{-11}$ $m^2 \cdot s^{-1}$, respectively, which correspond to $r_H^{uni} = 1.4 \pm 0.2$ nm and $r_H^{mic} = 5.6 \pm 0.9$ nm, respectively.

We conclude that the variation of the degree of polymerization of the hydrophilic block by a factor of ≈2 does not have an influence on any of the values determined. The CMC's of both triblock copolymers coincide as well, which is in agreement with previous findings on di- and triblock copolymers of ethylene oxide and propylene oxide where the CMC was found to be mainly dependent on the degree of polymerization of the hydrophobic block and only to a lesser extent on the degree of polymerization of the hydrophilic block.[21–23]

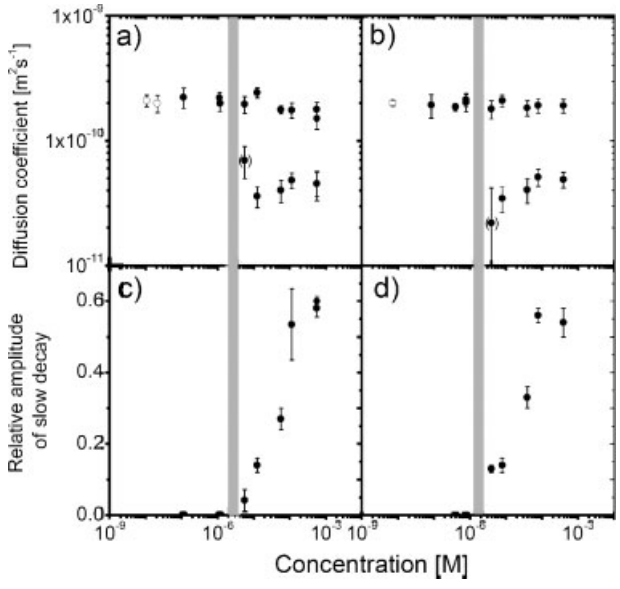

Figure 2. FCS results from $PMOx_{20}$-*b*-$PNOx_7$-*b*-$PMOx_{14}$ (a, c) and $PMOx_{30}$-*b*-$PNOx_7$-*b*-$PMOx_{26}$ (b, d) with the identical fluorescence-labeled copolymers as tracers in dependence on the overall copolymer concentration. (a, b) Concentration dependence of the diffusion coefficients and (c,d) the relative amplitudes of the slow decay. Open symbols: solutions containing fluorescence-labeled polymers only, closed symbols: solutions containing both labeled and non-labeled polymers. The concentration of labeled copolymers was kept below 10^{-8} M. The gray bars indicate the resulting CMCs. The uncertainties of the diffusion coefficients have been determined from repeated measurements (at least five). The data points in parentheses were not considered for the calculation of the average diffusion coefficients of the micelles.

Gradient Copolymers

Very similar aggregation behavior is observed with the random copolymer, $P(MOx_{40}$-*g*-$NOx_6)$ (Figure 3 and 4): The polymers are present as unimers at low concentrations, whereas unimers and micelles coexist at higher concentrations. The average diffusion coefficients of thelabeled unimers and micelles are $(2.1 \pm 0.2) \times 10^{-10}$ $m^2 \cdot s^{-1}$ and $(5.2 \pm 0.3) \times 10^{-11}$ $m^2 \cdot s^{-1}$, which corresponds to $r_H^{uni} = 1.2 \pm 0.1$ nm and $r_H^{mic} = 4.7 \pm 0.3$ nm. The CMC is found at 8×10^{-6} M, and the decrease of the relative amplitude of the slow decay is as pronounced as for the diblock and triblock copolymers.

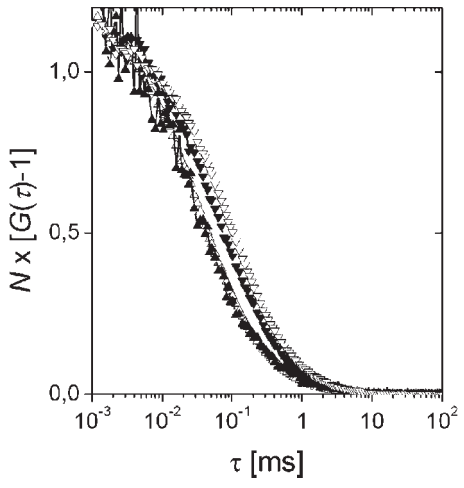

Figure 3. FCS correlation functions of aqueous solutions of the gradient copolymer $P(MOx_{40}$-*g*-$NOx_6)$ at the overall polymer concentrations 3×10^{-8} M (▲), 5×10^{-6} M (△), 1×10^{-4} M (▼) and 2×10^{-3} M (▽).

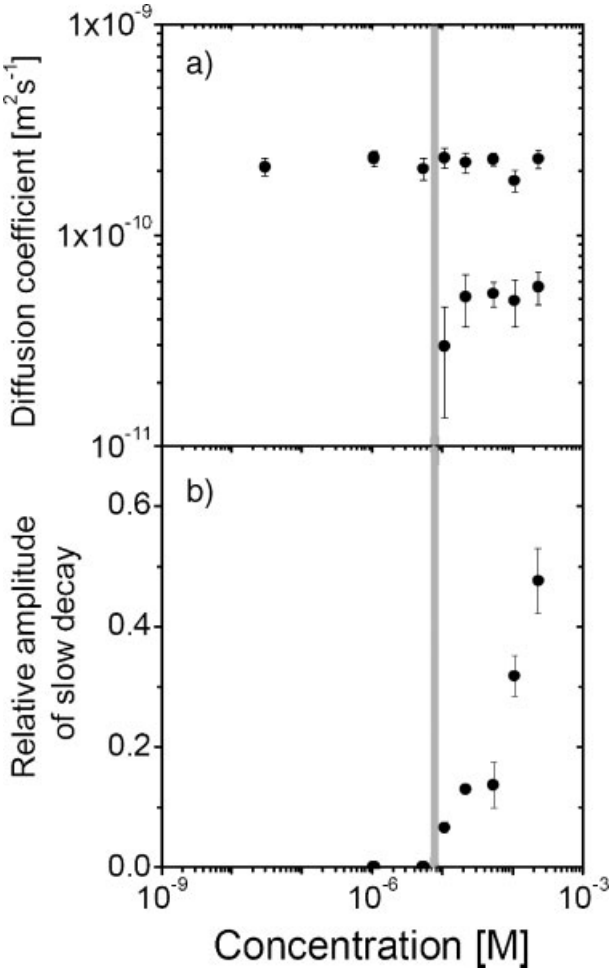

Figure 4. FCS results from P(MOx_{40}-*g*-NOx_6) with the identical fluorescence-labeled copolymers as tracers in dependence on the overall copolymer concentration. (a) Concentration dependence of the diffusion coefficients of P(MOx_{40}-*g*-NOx_6). All solutions contained both fluorescence-labeled and non-labeled polymers with the concentration of labeled copolymers below 3×10^{-8} M. (b) Relative amplitude of the slow decay. The gray bar indicates the resulting CMC.

Discussion

In this section, we compare the hydrodynamic radii of the unimers of the copolymers with the ones from the previously reported diblock copolymers[9] and from PMOx homopolymers. The dependence of the hydrodynamic radii of the micelles as well as the CMC's on the copolymer architecture is eventually discussed.

Hydrodynamic Radius of the Unimers

The hydrodynamic radii of poly(2-oxazoline) unimers are not easily accessible with classical techniques because micelles form at low concentrations already (the CMC's are as low as 10^{-5} M or even below), and their signal dominates over the signal from the unimers, e.g. in scattering experiments. FCS offers the possibility to measure the hydrodynamic radius of fluorescence-labeled polymers because concentrations far lower than the CMC can be accessed, where the autocorrelation curve is entirely due to unimers (apart from the fast triplet decay). Moreover, even above the CMC, the decay from the unimers can be distinguished from the one of the micelles.

We compare here the values of r_H^{uni} of poly(2-oxazoline) copolymers of different architecture to values from PMOx homopolymers having molar masses in the same range (see Figure 5a).[24] The comparison shows that the hydrodynamic radii of the copolymers are significantly smaller than the ones of the homopolymers having the same overall molar mass. We attribute this reduction of the hydrodynamic radius to the influence of the NOx monomers, which aggregate in aqueous solution, thus leading to less extended chain conformations for the copolymers. In the range studied, no dependence on the

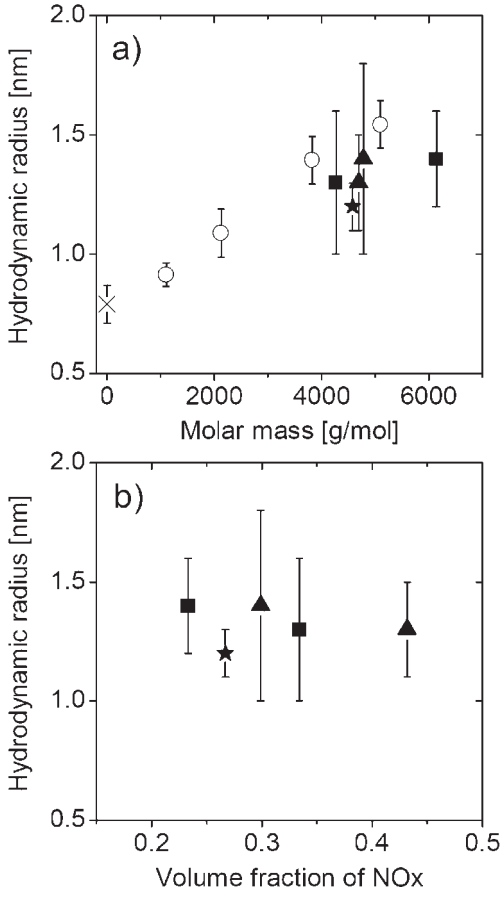

Figure 5. Hydrodynamic radii of the fluorescence-labeled unimers as a function of (a) overall molar mass and (b) f_{NOx}. (×) TRITC, (○) pMOx homopolymers, (▲) diblock copolymers, (■) triblock copolymers, (★) gradient copolymer.

Macromol. Chem. Phys. **2007**, *208*, 1402–1408

DOI: 10.1002/macp.200700140

volume fraction of NOx could be detected, though (Figure 5b).

Hydrodynamic Radii of the Micelles Formed by Triblock Copolymers

The hydrodynamic radii of the micelles formed by the triblock copolymers are roughly half the ones of the micelles formed by the diblock copolymers, independent of the degree of polymerization of the hydrophilic block (Table 1). The degrees of polymerization of the hydrophobic blocks in the triblock copolymers are very similar to those of the diblock copolymers. The origin of the reduction in size has several reasons: (i) The additional hindrance imposed by the architecture of the triblock copolymer: In micelles formed by triblock copolymers, both ends of the hydrophobic block are located near the surface of the micellar core, whereas the hydrophobic block stretches from the surface of the micellar core to the center (Figure 6a and b). (ii) The grafting density of hydrophilic blocks at the core surface: In the triblock copolymers, each hydrophobic block is bound to two hydrophilic blocks in triblock copolymers, whereas it is only bound to one hydrophilic block in diblock copolymers. (iii) For diblock copolymers, the micellar core must therefore contain more hydrophobic segments to stabilize the micelle and is thus larger than in the case of triblocks. These effects seem to dominate over the difference of the degrees of polymerization of the hydrophilic blocks of the two triblock copolymers under study.

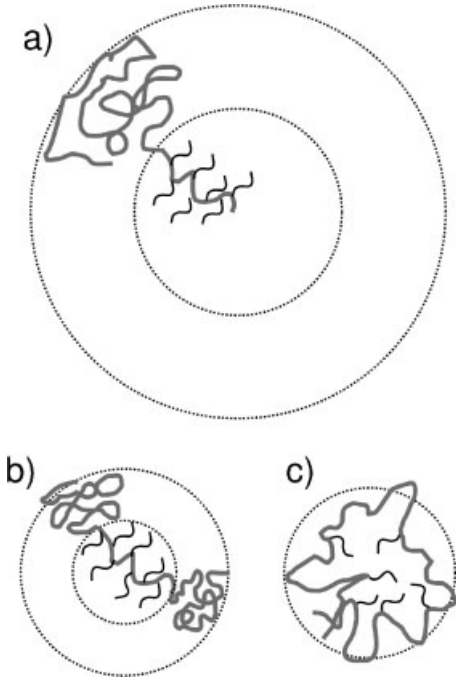

Figure 6. Sketch of the micelles formed by (a) diblock, (b) triblock and (c) gradient copolymers. The circles indicate the surface of the micellar core and the micellar shell, respectively. The thick gray lines represent the hydrophilic backbone, the thin black lines the nonyl side groups. For clarity, a single polymer is shown per micelle, even though they consist of a number of polymers.

Size of the Micelles Formed by Gradient Copolymers

The hydrodynamic radius of the micelles formed by the gradient copolymers calculate to 4.7 nm, i.e. even smaller than the one of the triblock copolymers. We do not expect the gradient copolymer to form micelles of distinct core-shell morphology because the hydrophobic and hydrophilic monomer units are not arranged in separated blocks. Possibly, the hydrophobic *n*-nonyl side groups aggregate with the polymer backbone partly wrapping around (Figure 6c). The contour length of the *n*-nonyl side groups can be estimated to be ≈1.0–1.2 nm.[25] The value $r_H^{mic} =$ 4.7 nm may thus result from aggregated, stretched *n*-nonyl side groups with the main chain wrapped around. However, we cannot exclude more complex structures. In this context, the results by Schulz[15] on random copolymers in bulk, showing no alkyl side chain melting transition, are corroborating our interpretation of a frustrated association of the alkyl side chains in the aggregates.

CMC's

The CMC's of the triblock copolymers are of the order of ($\approx 2 \times 10^{-6}$ M), i.e. lower than the ones of the diblock copolymers described in ref.[9] (10^{-5} M). This behavior is contradictory to what has been reported for block copolymers based on ethylene oxide (E) and butylene oxide (B) in aqueous solution:[26] In measurements of the surface tension, the CMC of a diblock copolymer with the composition $E_{41}B_8$ was found to be 1.3×10^{-4} M, whereas the one of a triblock copolymer $E_{21}B_8E_{21}$ is a factor of 10 higher. The same behavior was observed with block copolymers based on ethylene oxide and propylene oxide (P):[27] Static light scattering experiments resulted in a CMC of 1.2×10^{-4} M for a diblock copolymer $E_{102}P_{37}$ and 5×10^{-3} M for a triblock copolymer $E_{52}P_{34}E_{52}$. The different behavior of the poly(2-oxazoline) copolymers requires further research in order to identify the reasons.

The gradient copolymer, P(MOx_{40}-*g*-NOx_6), exhibits a CMC very close to the one of the diblock copolymer, although the size of the micelles formed by the gradient copolymers are smaller (Table 1). The relatively high CMC of the gradient copolymer may be attributed to a stabilization of the unimer state in solution by the intramolecular aggregation of the nonyl chains.

In a recent study, the effect of random and diblock copolymers from MOx and NOx on the surface tension of

water was investigated.[14] The copolymers had similar compositions, P(MOx_{29}-*r*-NOx_7) and $PMOx_{27}$-*b*-$PNOx_5$, which are in the same range as the ones in our study. The CMC's can be inferred from the drop of the surface tension between 10^{-6}–10^{-5} M, which corresponds very well to the CMC of the copolymers studied in the present work. However, the function of the surface tension vs. the polymer concentration did not allow the identification of a distinct CMC.

Conclusion

Fluorescence correlation spectroscopy is a very valuable tool to investigate the aggregation behavior of amphiphilic copolymers. By means of tracers that are identical to the copolymers under study, a large concentration range (10^{-8}–10^{-3} M) can be accessed. In this way, the CMC of various copolymers has been detected and reliable values for the hydrodynamic radii of the labeled unimers and micelles have been obtained. The architecture of the poly(2-oxazoline) copolymers composed of MOx and NOx monomers has a significant influence on the aggregation behavior: (i) The hydrodynamic radii of the unimers is decreased with respect to the ones of PMOx homopolymers, which we ascribe to association of the nonyl groups, even below the CMC. (ii) The CMC's are detected at concentrations of $\approx 10^{-5}$ M, however, in the present system, the CMC's of the triblock copolymers are lower than the ones of the diblock copolymers, in contrast to other amphiphilic systems described in the literature. (iii) The hydrodynamic radii of the micelles formed by the triblock copolymers are lower than the one of the diblock copolymers. We ascribe this behavior to the space demands of the hydrophilic block as well as the stretching of the core block through the micellar core. For gradient copolymers, the micellar hydrodynamic radii are even lower and constant up to 2 decades above the CMC. Importantly, the sensitive FCS technique revealed that gradient copolymers of 2-oxazolines display a distinct CMC.

Acknowledgements: We wish to thank *J. Rädler*, *S. Keller* and *J. Bayer*, Ludwig-Maximilians-Universität München, for providing the FCS instrument and for help with the measurements. We also gratefully acknowledge financial support by the *Deutsche Forschungsgemeinschaft* (Pa 771/2-1 and Jo 287/4-1).

Received: March 12, 2007; Revised: March 30, 2007; Accepted: April 4, 2007; DOI: 10.1002/macp.200700140

Keywords: polymer physics; amphiphilic copolymers; fluorescence correlation spectroscopy

[1] C. Price, in: *Developments in Block Copolymers*, I. Goodmann, Ed., Applied Science Publishers, London 1982, Vol. 1, p. 39.

[2] G. Riess, G. Hurtrez, P. Bahadur, in: *Encylopedia of Polymer Sciences and Engineering*, 2nd Edition, H. F. Mark, N. M. Bikales, C. G. Overberger, G. Menges, Eds., Wiley-Interscience, New York 1985, Vol. 2, p. 324.

[3] *Amphiphilic Block Copolymers: Self-Assembly and Applications*, P. Alexandridis, B. Lindman, Eds., Elsevier, Amsterdam 2000.

[4] G. Riess, *Prog. Polym. Sci.* **2003**, *28*, 1107.

[5] D. F. Evans, H. Wennerström, "*The Colloidal Domain*", Wiley-VCH, Weinheim 1999, p. 173.

[6] G. Wanka, H. Hoffmann, W. Ulbricht, *Macromolecules* **1994**, *27*, 4145.

[7] D. F. Siqueira, S. P. Nunes, B. A. Wolf, *Macromolecules* **1994**, *27*, 4561.

[8] K. Lüdtke, R. Jordan, P. Hommes, O. Nuyken, C. A. Naumann, *Macromol. Biosci.* **2005**, *5*, 384.

[9] [9a] T. B. Bonné, K. Lüdtke, R. Jordan, P. Štěpánek, C. M. Papadakis, *Colloid Polym. Sci.* **2004**, *282*, 833; [9b] T. B. Bonné, K. Lüdtke, R. Jordan, P. Štěpánek, C. M. Papadakis, *Colloid Polym. Sci.* **2004**, *282*, 1425.

[10] T. B. Bonné, K. Lüdtke, R. Jordan, C. M. Papadakis, *Colloid Polym. Sci.* **2007**, *5*, 491.

[11] T. Komenda, K. Lüdtke, R. Jordan, R. Ivanova, T. B. Bonné, C. M. Papadakis, *Polym. Prepr.* **2006**, *47*, 197.

[12] C. M. Papadakis, R. Ivanova, K. Lüdtke, K. Mortensen, P. K. Pranzas, R. Jordan, *J. Appl. Cryst.* **2007**, *40*, 361.

[13] R. Ivanova, T. B. Bonné, K. Lüdtke, T. Komenda, R. Jordan, K. Mortensen, C. M. Papadakis, to be published.

[14] M. Bortenschlager, N. Schöllhorn, A. Wittmann, R. Weberskirch, *Chem. Eur. J.* **2006**, *13*, 520.

[15] R. C. Schulz, *Makromol. Chem., Macromol. Symp.* **1993**, *73*, 103.

[16] R. Hoogenboom, M. W. Fijten, U. S. Schubert, *J. Polym. Sci., Part A: Polym. Chem.* **2004**, *42*, 1820.

[17] R. Luxenhofer, R. Jordan, *Macromolecules* **2006**, *39*, 3509.

[18] S. Cesana, J. Auernheimer, R. Jordan, H. Kessler, O. Nuyken, *Macromol. Chem. Phys.* **2006**, *207*, 183.

[19] J. Widengren, Ü. Mets, R. Rigler, *J. Phys. Chem.* **1995**, *99*, 13368.

[20] D. Magde, E. L. Elson, W. W. Webb, *Biopolymers* **1974**, *13*, 29.

[21] P. Alexandridis, J. F. Holzwartz, T. A. Hatton, *Macromolecules* **1994**, *27*, 2414.

[22] J. R. Lopes, W. Loh, *Langmuir* **1998**, *14*, 750.

[23] A. Kelaraks, Z. Yang, E. Pousia, S. K. Nixon, C. Price, C. Booth, I. W. Hamley, V. Castelletto, J. Fundin, *Langmuir* **2001**, *17*, 8085.

[24] T. B. Bonné, PhD thesis, Technische Universität München 2006.

[25] CS Chem 3D ultra 7.0. 0.

[26] Z. Yang, S. Pickard, N.-J. Deng, R. J. Barlow, D. Attwood, C. Booth, *Macromolecules* **1994**, *27*, 2371.

[27] H. Altinok, G.-E. Yu, K. Nixon, P. A. Gorry, D. Attwood, C. Booth, *Langmuir* **1997**, *13*, 5837.

[28] D. W. van Krevelen, in: *Properties of Polymers*, Elsevier, Amsterdam 1990, p. 71.

[29] M. Litt, F. Rahl, L. G. Roldan, *J. Polym. Sci. A-2* **1969**, *7*, 463.